

Observation of $e^+e^- \rightarrow \pi^0\pi^0\psi_2(3823)$

The BESIII Collaboration



M. Ablikim¹, M. N. Achasov^{11,b}, P. Adlarson⁷⁰, M. Albrecht⁴, R. Aliberti³¹,
A. Amoroso^{69A,69C}, M. R. An³⁵, Q. An^{66,53}, X. H. Bai⁶¹, Y. Bai⁵², O. Bakina³²,
R. Baldini Ferrolli^{26A}, I. Balossino^{27A}, Y. Ban^{42,g}, V. Batozskaya^{1,40}, D. Becker³¹,
K. Begzsuren²⁹, N. Berger³¹, M. Bertani^{26A}, D. Bettoni^{27A}, F. Bianchi^{69A,69C},
J. Bloms⁶³, A. Bortone^{69A,69C}, I. Boyko³², R. A. Briere⁵, A. Brueggemann⁶³, H. Cai⁷¹,
X. Cai^{1,53}, A. Calcaterra^{26A}, G. F. Cao^{1,58}, N. Cao^{1,58}, S. A. Cetin^{57A}, J. F. Chang^{1,53},
W. L. Chang^{1,58}, G. R. Che³⁹, G. Chelkov^{32,a}, C. Chen³⁹, Chao Chen⁵⁰, G. Chen¹,
H. S. Chen^{1,58}, M. L. Chen^{1,53}, S. J. Chen³⁸, S. M. Chen⁵⁶, T. Chen¹, X. R. Chen^{28,58},
X. T. Chen¹, Y. B. Chen^{1,53}, Z. J. Chen^{23,h}, W. S. Cheng^{69C}, S. K. Choi⁵⁰, X. Chu³⁹,
G. Cibinetto^{27A}, F. Cossio^{69C}, J. J. Cui⁴⁵, H. L. Dai^{1,53}, J. P. Dai⁷³, A. Dbeyssi¹⁷,
R. E. de Boer⁴, D. Dedovich³², Z. Y. Deng¹, A. Denig³¹, I. Denysenko³²,
M. Destefanis^{69A,69C}, F. De Mori^{69A,69C}, Y. Ding³⁶, J. Dong^{1,53}, L. Y. Dong^{1,58},
M. Y. Dong^{1,53,58}, X. Dong⁷¹, S. X. Du⁷⁵, P. Egorov^{32,a}, Y. L. Fan⁷¹, J. Fang^{1,53},
S. S. Fang^{1,58}, W. X. Fang¹, Y. Fang¹, R. Farinelli^{27A}, L. Fava^{69B,69C}, F. Feldbauer⁴,
G. Felici^{26A}, C. Q. Feng^{66,53}, J. H. Feng⁵⁴, K. Fischer⁶⁴, M. Fritsch⁴, C. Fritzsche⁶³,
C. D. Fu¹, H. Gao⁵⁸, Y. N. Gao^{42,g}, Yang Gao^{66,53}, S. Garbolino^{69C}, I. Garzia^{27A,27B},
P. T. Ge⁷¹, Z. W. Ge³⁸, C. Geng⁵⁴, E. M. Gersabeck⁶², A. Gilman⁶⁴, K. Goetzen¹²,
L. Gong³⁶, W. X. Gong^{1,53}, W. Gradl³¹, M. Greco^{69A,69C}, L. M. Gu³⁸, M. H. Gu^{1,53},
Y. T. Gu¹⁴, C. Y. Guan^{1,58}, A. Q. Guo^{28,58}, L. B. Guo³⁷, R. P. Guo⁴⁴, Y. P. Guo^{10,f},
A. Guskov^{32,a}, T. T. Han⁴⁵, W. Y. Han³⁵, X. Q. Hao¹⁸, F. A. Harris⁶⁰, K. K. He⁵⁰,
K. L. He^{1,58}, F. H. Heinsius⁴, C. H. Heinz³¹, Y. K. Heng^{1,53,58}, C. Herold⁵⁵,
G. Y. Hou^{1,58}, Y. R. Hou⁵⁸, Z. L. Hou¹, H. M. Hu^{1,58}, J. F. Hu^{51,i}, T. Hu^{1,53,58},
Y. Hu¹, G. S. Huang^{66,53}, K. X. Huang⁵⁴, L. Q. Huang^{28,58}, X. T. Huang⁴⁵,
Y. P. Huang¹, Z. Huang^{42,g}, T. Hussain⁶⁸, N. Hüsken^{25,31}, W. Imoehl²⁵, M. Irshad^{66,53},
J. Jackson²⁵, S. Jaeger⁴, S. Janchiv²⁹, E. Jang⁵⁰, J. H. Jeong⁵⁰, Q. Ji¹, Q. P. Ji¹⁸,
X. B. Ji^{1,58}, X. L. Ji^{1,53}, Y. Y. Ji⁴⁵, Z. K. Jia^{66,53}, H. B. Jiang⁴⁵, S. S. Jiang³⁵,
X. S. Jiang^{1,53,58}, Y. Jiang⁵⁸, J. B. Jiao⁴⁵, Z. Jiao²¹, S. Jin³⁸, Y. Jin⁶¹, M. Q. Jing^{1,58},
T. Johansson⁷⁰, N. Kalantar-Nayestanaki⁵⁹, X. S. Kang³⁶, R. Kappert⁵⁹,
M. Kavatsyuk⁵⁹, B. C. Ke⁷⁵, I. K. Keshk⁴, A. Khoukaz⁶³, R. Kiuchi¹, R. Kliemt¹²,
L. Koch³³, O. B. Kolcu^{57A}, B. Kopf⁴, M. Kuemmel⁴, M. Kuessner⁴, A. Kupsc^{40,70},
W. Kühn³³, J. J. Lane⁶², J. S. Lange³³, P. Larin¹⁷, A. Lavanaia²⁴, L. Lavezzi^{69A,69C},
Z. H. Lei^{66,53}, H. Leithoff³¹, M. Lellmann³¹, T. Lenz³¹, C. Li³⁹, C. Li⁴³, C. H. Li³⁵,

Cheng Li^{66,53}, D. M. Li⁷⁵, F. Li^{1,53}, G. Li¹, H. Li^{66,53}, H. Li⁴⁷, H. B. Li^{1,58}, H. J. Li¹⁸,
H. N. Li^{51,i}, J. Q. Li⁴, J. S. Li⁵⁴, J. W. Li⁴⁵, Ke Li¹, L. J. Li¹, L. K. Li¹, Lei Li³,
M. H. Li³⁹, P. R. Li^{34,j,k}, S. X. Li¹⁰, S. Y. Li⁵⁶, T. Li⁴⁵, W. D. Li^{1,58}, W. G. Li¹,
X. H. Li^{66,53}, X. L. Li⁴⁵, Xiaoyu Li^{1,58}, Y. G. Li^{42,g}, Z. X. Li¹⁴, Z. Y. Li⁵⁴, H. Liang^{1,58},
H. Liang³⁰, H. Liang^{66,53}, Y. F. Liang⁴⁹, Y. T. Liang^{28,58}, G. R. Liao¹³, L. Z. Liao⁴⁵,
J. Libby²⁴, A. Limphirat⁵⁵, C. X. Lin⁵⁴, D. X. Lin^{28,58}, T. Lin¹, B. J. Liu¹, C. X. Liu¹,
D. Liu^{17,66}, F. H. Liu⁴⁸, Fang Liu¹, Feng Liu⁶, G. M. Liu^{51,i}, H. Liu^{34,j,k}, H. B. Liu¹⁴,
H. M. Liu^{1,58}, Huanhuan Liu¹, Huihui Liu¹⁹, J. B. Liu^{66,53}, J. L. Liu⁶⁷, J. Y. Liu^{1,58},
K. Liu¹, K. Y. Liu³⁶, Ke Liu²⁰, L. Liu^{66,53}, Lu Liu³⁹, M. H. Liu^{10,f}, P. L. Liu¹, Q. Liu⁵⁸,
S. B. Liu^{66,53}, T. Liu^{10,f}, W. K. Liu³⁹, W. M. Liu^{66,53}, X. Liu^{34,j,k}, Y. Liu^{34,j,k},
Y. B. Liu³⁹, Z. A. Liu^{1,53,58}, Z. Q. Liu⁴⁵, X. C. Lou^{1,53,58}, F. X. Lu⁵⁴, H. J. Lu²¹,
J. G. Lu^{1,53}, X. L. Lu¹, Y. Lu⁷, Y. P. Lu^{1,53}, Z. H. Lu¹, C. L. Luo³⁷, M. X. Luo⁷⁴,
T. Luo^{10,f}, X. L. Luo^{1,53}, X. R. Lyu⁵⁸, Y. F. Lyu³⁹, F. C. Ma³⁶, H. L. Ma¹,
L. L. Ma⁴⁵, M. M. Ma^{1,58}, Q. M. Ma¹, R. Q. Ma^{1,58}, R. T. Ma⁵⁸, X. Y. Ma^{1,53},
Y. Ma^{42,g}, F. E. Maas¹⁷, M. Maggiora^{69A,69C}, S. Maldaner⁴, S. Malde⁶⁴,
Q. A. Malik⁶⁸, A. Mangoni^{26B}, Y. J. Mao^{42,g}, Z. P. Mao¹, S. Marcello^{69A,69C},
Z. X. Meng⁶¹, J. Messchendorp^{12,59}, G. Mezzadri^{27A}, H. Miao¹, T. J. Min³⁸,
R. E. Mitchell²⁵, X. H. Mo^{1,53,58}, N. Yu. Muchnoi^{11,b}, Y. Nefedov³², F. Nerling^{17,d},
I. B. Nikolaev^{11,b}, Z. Ning^{1,53}, S. Nisar^{9,l}, Y. Niu⁴⁵, S. L. Olsen⁵⁸, Q. Ouyang^{1,53,58},
S. Pacetti^{26B,26C}, X. Pan^{10,f}, Y. Pan⁵², A. Pathak³⁰, M. Pelizaeus⁴, H. P. Peng^{66,53},
K. Peters^{12,d}, J. L. Ping³⁷, R. G. Ping^{1,58}, S. Plura³¹, S. Pogodin³², V. Prasad^{66,53},
F. Z. Qi¹, H. Qi^{66,53}, H. R. Qi⁵⁶, M. Qi³⁸, T. Y. Qi^{10,f}, S. Qian^{1,53}, W. B. Qian⁵⁸,
Z. Qian⁵⁴, C. F. Qiao⁵⁸, J. J. Qin⁶⁷, L. Q. Qin¹³, X. P. Qin^{10,f}, X. S. Qin⁴⁵,
Z. H. Qin^{1,53}, J. F. Qiu¹, S. Q. Qu⁵⁶, K. H. Rashid⁶⁸, C. F. Redmer³¹, K. J. Ren³⁵,
A. Rivetti^{69C}, V. Rodin⁵⁹, M. Rolo^{69C}, G. Rong^{1,58}, Ch. Rosner¹⁷, S. N. Ruan³⁹,
H. S. Sang⁶⁶, A. Sarantsev^{32,c}, Y. Schelhaas³¹, C. Schnier⁴, K. Schoenning⁷⁰,
M. Scodreggio^{27A,27B}, K. Y. Shan^{10,f}, W. Shan²², X. Y. Shan^{66,53}, J. F. Shangguan⁵⁰,
L. G. Shao^{1,58}, M. Shao^{66,53}, C. P. Shen^{10,f}, H. F. Shen^{1,58}, X. Y. Shen^{1,58},
B. A. Shi⁵⁸, H. C. Shi^{66,53}, J. Y. Shi¹, q. q. Shi⁵⁰, R. S. Shi^{1,58}, X. Shi^{1,53},
X. D. Shi^{66,53}, J. J. Song¹⁸, W. M. Song^{30,1}, Y. X. Song^{42,g}, S. Sosio^{69A,69C},
S. Spataro^{69A,69C}, F. Stieler³¹, K. X. Su⁷¹, P. P. Su⁵⁰, Y. J. Su⁵⁸, G. X. Sun¹,
H. Sun⁵⁸, H. K. Sun¹, J. F. Sun¹⁸, L. Sun⁷¹, S. S. Sun^{1,58}, T. Sun^{1,58}, W. Y. Sun³⁰,
X. Sun^{23,h}, Y. J. Sun^{66,53}, Y. Z. Sun¹, Z. T. Sun⁴⁵, Y. H. Tan⁷¹, Y. X. Tan^{66,53},
C. J. Tang⁴⁹, G. Y. Tang¹, J. Tang⁵⁴, L. Y. Tao⁶⁷, Q. T. Tao^{23,h}, M. Tat⁶⁴,
J. X. Teng^{66,53}, V. Thoren⁷⁰, W. H. Tian⁴⁷, Y. Tian^{28,58}, I. Uman^{57B}, B. Wang¹,
B. L. Wang⁵⁸, C. W. Wang³⁸, D. Y. Wang^{42,g}, F. Wang⁶⁷, H. J. Wang^{34,j,k},
H. P. Wang^{1,58}, K. Wang^{1,53}, L. L. Wang¹, M. Wang⁴⁵, M. Z. Wang^{42,g},
Meng Wang^{1,58}, S. Wang^{10,f}, S. Wang¹³, T. Wang^{10,f}, T. J. Wang³⁹, W. Wang⁵⁴,
W. H. Wang⁷¹, W. P. Wang^{66,53}, X. Wang^{42,g}, X. F. Wang^{34,j,k}, X. L. Wang^{10,f},
Y. Wang⁵⁶, Y. D. Wang⁴¹, Y. F. Wang^{1,53,58}, Y. H. Wang⁴³, Y. Q. Wang¹,
Yaqian Wang^{16,1}, Z. Wang^{1,53}, Z. Y. Wang^{1,58}, Ziyi Wang⁵⁸, D. H. Wei¹³,
F. Weidner⁶³, S. P. Wen¹, D. J. White⁶², U. Wiedner⁴, G. Wilkinson⁶⁴, M. Wolke⁷⁰,
L. Wollenberg⁴, J. F. Wu^{1,58}, L. H. Wu¹, L. J. Wu^{1,58}, X. Wu^{10,f}, X. H. Wu³⁰,

Y. Wu⁶⁶, Y. J. Wu²⁸, Z. Wu^{1,53}, L. Xia^{66,53}, T. Xiang^{42,g}, D. Xiao^{34,j,k}, G. Y. Xiao³⁸, H. Xiao^{10,f}, S. Y. Xiao¹, Y. L. Xiao^{10,f}, Z. J. Xiao³⁷, C. Xie³⁸, X. H. Xie^{42,g}, Y. Xie⁴⁵, Y. G. Xie^{1,53}, Y. H. Xie⁶, Z. P. Xie^{66,53}, T. Y. Xing^{1,58}, C. F. Xu¹, C. J. Xu⁵⁴, G. F. Xu¹, H. Y. Xu⁶¹, Q. J. Xu¹⁵, X. P. Xu⁵⁰, Y. C. Xu⁵⁸, Z. P. Xu³⁸, F. Yan^{10,f}, L. Yan^{10,f}, W. B. Yan^{66,53}, W. C. Yan⁷⁵, H. J. Yang^{46,e}, H. L. Yang³⁰, H. X. Yang¹, L. Yang⁴⁷, S. L. Yang⁵⁸, Tao Yang¹, Y. F. Yang³⁹, Y. X. Yang^{1,58}, Yifan Yang^{1,58}, M. Ye^{1,53}, M. H. Ye⁸, J. H. Yin¹, Z. Y. You⁵⁴, B. X. Yu^{1,53,58}, C. X. Yu³⁹, G. Yu^{1,58}, T. Yu⁶⁷, X. D. Yu^{42,g}, C. Z. Yuan^{1,58}, L. Yuan², S. C. Yuan¹, X. Q. Yuan¹, Y. Yuan^{1,58}, Z. Y. Yuan⁵⁴, C. X. Yue³⁵, A. A. Zafar⁶⁸, F. R. Zeng⁴⁵, X. Zeng⁶, Y. Zeng^{23,h}, Y. H. Zhan⁵⁴, A. Q. Zhang¹, B. L. Zhang¹, B. X. Zhang¹, D. H. Zhang³⁹, G. Y. Zhang¹⁸, H. Zhang⁶⁶, H. H. Zhang³⁰, H. H. Zhang⁵⁴, H. Y. Zhang^{1,53}, J. L. Zhang⁷², J. Q. Zhang³⁷, J. W. Zhang^{1,53,58}, J. X. Zhang^{34,j,k}, J. Y. Zhang¹, J. Z. Zhang^{1,58}, Jianyu Zhang^{1,58}, Jiawei Zhang^{1,58}, L. M. Zhang⁵⁶, L. Q. Zhang⁵⁴, Lei Zhang³⁸, P. Zhang¹, Q. Y. Zhang^{35,75}, Shuihan Zhang^{1,58}, Shulei Zhang^{23,h}, X. D. Zhang⁴¹, X. M. Zhang¹, X. Y. Zhang⁴⁵, X. Y. Zhang⁵⁰, Y. Zhang⁶⁴, Y. T. Zhang⁷⁵, Y. H. Zhang^{1,53}, Yan Zhang^{66,53}, Yao Zhang¹, Z. H. Zhang¹, Z. Y. Zhang³⁹, Z. Y. Zhang⁷¹, G. Zhao¹, J. Zhao³⁵, J. Y. Zhao^{1,58}, J. Z. Zhao^{1,53}, Lei Zhao^{66,53}, Ling Zhao¹, M. G. Zhao³⁹, S. J. Zhao⁷⁵, Y. B. Zhao^{1,53}, Y. X. Zhao^{28,58}, Z. G. Zhao^{66,53}, A. Zhemchugov^{32,a}, B. Zheng⁶⁷, J. P. Zheng^{1,53}, Y. H. Zheng⁵⁸, B. Zhong³⁷, C. Zhong⁶⁷, X. Zhong⁵⁴, H. Zhou⁴⁵, L. P. Zhou^{1,58}, X. Zhou⁷¹, X. K. Zhou⁵⁸, X. R. Zhou^{66,53}, X. Y. Zhou³⁵, Y. Z. Zhou^{10,f}, J. Zhu³⁹, K. Zhu¹, K. J. Zhu^{1,53,58}, L. X. Zhu⁵⁸, S. H. Zhu⁶⁵, S. Q. Zhu³⁸, T. J. Zhu⁷², W. J. Zhu^{10,f}, Y. C. Zhu^{66,53}, Z. A. Zhu^{1,58}, J. H. Zou¹

¹ Institute of High Energy Physics, Beijing 100049, People's Republic of China

² Beihang University, Beijing 100191, People's Republic of China

³ Beijing Institute of Petrochemical Technology, Beijing 102617, People's Republic of China

⁴ Bochum Ruhr-University, D-44780 Bochum, Germany

⁵ Carnegie Mellon University, Pittsburgh, Pennsylvania 15213, USA

⁶ Central China Normal University, Wuhan 430079, People's Republic of China

⁷ Central South University, Changsha 410083, People's Republic of China

⁸ China Center of Advanced Science and Technology, Beijing 100190, People's Republic of China

⁹ COMSATS University Islamabad, Lahore Campus, Defence Road, Off Raiwind Road, 54000 Lahore, Pakistan

¹⁰ Fudan University, Shanghai 200433, People's Republic of China

¹¹ G.I. Budker Institute of Nuclear Physics SB RAS (BINP), Novosibirsk 630090, Russia

¹² GSI Helmholtzcentre for Heavy Ion Research GmbH, D-64291 Darmstadt, Germany

¹³ Guangxi Normal University, Guilin 541004, People's Republic of China

¹⁴ Guangxi University, Nanning 530004, People's Republic of China

¹⁵ Hangzhou Normal University, Hangzhou 310036, People's Republic of China

¹⁶ Hebei University, Baoding 071002, People's Republic of China

¹⁷ Helmholtz Institute Mainz, Staudinger Weg 18, D-55099 Mainz, Germany

¹⁸ Henan Normal University, Xinxiang 453007, People's Republic of China

¹⁹ Henan University of Science and Technology, Luoyang 471003, People's Republic of China

²⁰ Henan University of Technology, Zhengzhou 450001, People's Republic of China

- ²¹ *Huangshan College, Huangshan 245000, People's Republic of China*
- ²² *Hunan Normal University, Changsha 410081, People's Republic of China*
- ²³ *Hunan University, Changsha 410082, People's Republic of China*
- ²⁴ *Indian Institute of Technology Madras, Chennai 600036, India*
- ²⁵ *Indiana University, Bloomington, Indiana 47405, USA*
- ²⁶ *INFN Laboratori Nazionali di Frascati , (A)INFN Laboratori Nazionali di Frascati, I-00044, Frascati, Italy; (B)INFN Sezione di Perugia, I-06100, Perugia, Italy; (C)University of Perugia, I-06100, Perugia, Italy*
- ²⁷ *INFN Sezione di Ferrara, (A)INFN Sezione di Ferrara, I-44122, Ferrara, Italy; (B)University of Ferrara, I-44122, Ferrara, Italy*
- ²⁸ *Institute of Modern Physics, Lanzhou 730000, People's Republic of China*
- ²⁹ *Institute of Physics and Technology, Peace Avenue 54B, Ulaanbaatar 13330, Mongolia*
- ³⁰ *Jilin University, Changchun 130012, People's Republic of China*
- ³¹ *Johannes Gutenberg University of Mainz, Johann-Joachim-Becher-Weg 45, D-55099 Mainz, Germany*
- ³² *Joint Institute for Nuclear Research, 141980 Dubna, Moscow region, Russia*
- ³³ *Justus-Liebig-Universitaet Giessen, II. Physikalisches Institut, Heinrich-Buff-Ring 16, D-35392 Giessen, Germany*
- ³⁴ *Lanzhou University, Lanzhou 730000, People's Republic of China*
- ³⁵ *Liaoning Normal University, Dalian 116029, People's Republic of China*
- ³⁶ *Liaoning University, Shenyang 110036, People's Republic of China*
- ³⁷ *Nanjing Normal University, Nanjing 210023, People's Republic of China*
- ³⁸ *Nanjing University, Nanjing 210093, People's Republic of China*
- ³⁹ *Nankai University, Tianjin 300071, People's Republic of China*
- ⁴⁰ *National Centre for Nuclear Research, Warsaw 02-093, Poland*
- ⁴¹ *North China Electric Power University, Beijing 102206, People's Republic of China*
- ⁴² *Peking University, Beijing 100871, People's Republic of China*
- ⁴³ *Qufu Normal University, Qufu 273165, People's Republic of China*
- ⁴⁴ *Shandong Normal University, Jinan 250014, People's Republic of China*
- ⁴⁵ *Shandong University, Jinan 250100, People's Republic of China*
- ⁴⁶ *Shanghai Jiao Tong University, Shanghai 200240, People's Republic of China*
- ⁴⁷ *Shanxi Normal University, Linfen 041004, People's Republic of China*
- ⁴⁸ *Shanxi University, Taiyuan 030006, People's Republic of China*
- ⁴⁹ *Sichuan University, Chengdu 610064, People's Republic of China*
- ⁵⁰ *Soochow University, Suzhou 215006, People's Republic of China*
- ⁵¹ *South China Normal University, Guangzhou 510006, People's Republic of China*
- ⁵² *Southeast University, Nanjing 211100, People's Republic of China*
- ⁵³ *State Key Laboratory of Particle Detection and Electronics, Beijing 100049, Hefei 230026, People's Republic of China*
- ⁵⁴ *Sun Yat-Sen University, Guangzhou 510275, People's Republic of China*
- ⁵⁵ *Suranaree University of Technology, University Avenue 111, Nakhon Ratchasima 30000, Thailand*
- ⁵⁶ *Tsinghua University, Beijing 100084, People's Republic of China*
- ⁵⁷ *Turkish Accelerator Center Particle Factory Group, (A)Istinye University, 34010, Istanbul, Turkey; (B)Near East University, Nicosia, North Cyprus, Mersin 10, Turkey*
- ⁵⁸ *University of Chinese Academy of Sciences, Beijing 100049, People's Republic of China*
- ⁵⁹ *University of Groningen, NL-9747 AA Groningen, The Netherlands*
- ⁶⁰ *University of Hawaii, Honolulu, Hawaii 96822, USA*

- ⁶¹ *University of Jinan, Jinan 250022, People's Republic of China*
⁶² *University of Manchester, Oxford Road, Manchester, M13 9PL, United Kingdom*
⁶³ *University of Muenster, Wilhelm-Klemm-Strasse 9, 48149 Muenster, Germany*
⁶⁴ *University of Oxford, Keble Road, Oxford OX13RH, United Kingdom*
⁶⁵ *University of Science and Technology Liaoning, Anshan 114051, People's Republic of China*
⁶⁶ *University of Science and Technology of China, Hefei 230026, People's Republic of China*
⁶⁷ *University of South China, Hengyang 421001, People's Republic of China*
⁶⁸ *University of the Punjab, Lahore-54590, Pakistan*
⁶⁹ *University of Turin and INFN, (A)University of Turin, I-10125, Turin, Italy; (B)University of Eastern Piedmont, I-15121, Alessandria, Italy; (C)INFN, I-10125, Turin, Italy*
⁷⁰ *Uppsala University, Box 516, SE-75120 Uppsala, Sweden*
⁷¹ *Wuhan University, Wuhan 430072, People's Republic of China*
⁷² *Xinyang Normal University, Xinyang 464000, People's Republic of China*
⁷³ *Yunnan University, Kunming 650500, People's Republic of China*
⁷⁴ *Zhejiang University, Hangzhou 310027, People's Republic of China*
⁷⁵ *Zhengzhou University, Zhengzhou 450001, People's Republic of China*

- ^a *Also at the Moscow Institute of Physics and Technology, Moscow 141700, Russia*
^b *Also at the Novosibirsk State University, Novosibirsk, 630090, Russia*
^c *Also at the NRC "Kurchatov Institute", PNPI, 188300, Gatchina, Russia*
^d *Also at Goethe University Frankfurt, 60323 Frankfurt am Main, Germany*
^e *Also at Key Laboratory for Particle Physics, Astrophysics and Cosmology, Ministry of Education; Shanghai Key Laboratory for Particle Physics and Cosmology; Institute of Nuclear and Particle Physics, Shanghai 200240, People's Republic of China*
^f *Also at Key Laboratory of Nuclear Physics and Ion-beam Application (MOE) and Institute of Modern Physics, Fudan University, Shanghai 200443, People's Republic of China*
^g *Also at State Key Laboratory of Nuclear Physics and Technology, Peking University, Beijing 100871, People's Republic of China*
^h *Also at School of Physics and Electronics, Hunan University, Changsha 410082, China*
ⁱ *Also at Guangdong Provincial Key Laboratory of Nuclear Science, Institute of Quantum Matter, South China Normal University, Guangzhou 510006, China*
^j *Also at Frontiers Science Center for Rare Isotopes, Lanzhou University, Lanzhou 730000, People's Republic of China*
^k *Also at Lanzhou Center for Theoretical Physics, Lanzhou University, Lanzhou 730000, People's Republic of China*
^l *Also at the Department of Mathematical Sciences, IBA, Karachi, Pakistan*

E-mail: besiii-publications@ihep.ac.cn

ABSTRACT: Using a data sample corresponding to an integrated luminosity of 11.3 fb^{-1} collected at center-of-mass energies from 4.23 to 4.70 GeV with the BESIII detector, we observe the process $e^+e^- \rightarrow \pi^0\pi^0\psi_2(3823)$ for the first time with a statistical significance of 6.0σ . The ratio of average cross sections for $e^+e^- \rightarrow \pi^0\pi^0\psi_2(3823)$ over $\pi^+\pi^-\psi_2(3823)$ is determined to be $\mathcal{R} = \frac{\sigma[e^+e^- \rightarrow \pi^0\pi^0\psi_2(3823)]}{\sigma[e^+e^- \rightarrow \pi^+\pi^-\psi_2(3823)]} = 0.57 \pm 0.14 \pm 0.05$, which is consistent with expectations from isospin symmetry. Here and below, the first uncertainties are statistical and the second are systematic. The mass of the $\psi_2(3823)$ is measured to be $M[\psi_2(3823)] = 3824.5 \pm 2.4 \pm 1.0 \text{ MeV}/c^2$. Due to the limited statistics, the intrinsic width of the $\psi_2(3823)$ is measured as an upper limit of 18.8 MeV at 90% confidence level.

Contents

| | | |
|----------|--|----------|
| 1 | Introduction | 1 |
| 2 | BESIII detector and Monte Carlo simulation | 2 |
| 3 | Event selection and background study | 3 |
| 4 | Measurements of the mass and width of the $\psi_2(3823)$ | 4 |
| 5 | Measurement of the ratio of average cross sections | 5 |
| 6 | Systematic uncertainty | 6 |
| 7 | Summary and discussion | 7 |

1 Introduction

The study of exotic hadrons, whose quark contents are different from conventional baryons and mesons, remains an interesting topic in the field of hadron physics. In recent years, more than a dozen XYZ particles, which are considered to be good candidates for exotic hadrons [1, 2], have been discovered in the heavy quarkonium energy region. Here we discuss the Y -states, which appear as peaks in the center-of-mass energy dependence of e^+e^- cross sections. The first candidate, the $Y(4260)$, was discovered by the BaBar experiment in the Initial-State-Radiation (ISR) process $e^+e^- \rightarrow \gamma_{\text{ISR}}\pi^+\pi^-J/\psi$ [3], and later confirmed by the Belle experiment in the same process [4]. By studying the $e^+e^- \rightarrow \gamma_{\text{ISR}}\pi^+\pi^-\psi(2S)$ process, the BaBar experiment observed a new resonance, the $Y(4360)$ [5]. A detailed study with higher statistics by the Belle experiment confirmed the $Y(4360)$ resonance, and announced the discovery of a new resonance, the $Y(4660)$ [6]. An updated measurement by the BaBar experiment later confirmed the $Y(4660)$ resonance [7]. Since the Y -states are produced in direct e^+e^- annihilation or via its ISR process, they have the quantum numbers $J^{PC} = 1^{--}$, i.e., they are vector states. From the potential model, the vector charmonium states above the open-charm threshold are expected to decay dominantly to $D^{(*)}\bar{D}^{(*)}$ pairs [8]. However, as discussed above, these vector Y -states are widely discovered in hidden-charm final states, which indicates that they might be exotic states. To better understand their underlying nature, more experimental observations are desirable. Recently, the BESIII experiment reported the observation of resonance structures in the cross section measurement of the process $e^+e^- \rightarrow \pi^+\pi^-\psi_2(3823)$ [10], which suggests that the $\psi_2(3823)$ can be used as a probe for the study of Y -states.

Since its discovery in 1974 [11], the charmonium system has been considered an ideal environment in which to test quantum chromodynamics (QCD) in the non-perturbative

regime [12]. Just above the open-charm threshold, the $J = 2$ member of the D -wave spin-triplet, the 1^3D_2 charmonium state [aka the $\psi_2(3823)$], was studied by the E705, Belle, BESIII and LHCb experiments [13–16]. A recent measurement of the $\psi_2(3823)$ mass was reported by the BESIII experiment in the process $e^+e^- \rightarrow \pi^+\pi^-\psi_2(3823)$ [10]. More detailed measurements of $\psi_2(3823)$ properties were also performed at BESIII [17], but only 4.3σ evidence was found for the isospin neutral production process $e^+e^- \rightarrow \pi^0\pi^0\psi_2(3823)$. Moreover, there is still no direct measurement for the J^P of the $\psi_2(3823)$ at present. Further experimental constraints on its quantum numbers would improve our understanding of the $\psi_2(3823)$ and charmonium spectroscopy above open-charm threshold.

In this article, we perform a search for the process $e^+e^- \rightarrow \pi^0\pi^0\psi_2(3823)$ at BESIII by employing a partial-reconstruction method with a signal efficiency which is much higher than that of Ref. [17]. The ratio of average cross sections for $e^+e^- \rightarrow \pi^0\pi^0\psi_2(3823)$ over $e^+e^- \rightarrow \pi^+\pi^-\psi_2(3823)$ and the resonance parameters of the $\psi_2(3823)$ are also measured. The data sample, corresponding to an integrated luminosity of 11.3 fb^{-1} , was taken at center-of-mass (CM) energies from $\sqrt{s} = 4.23$ to 4.70 GeV [18] with the BESIII detector [19] operating at the Beijing Electron Positron Collider (BEPCII) [20]. The $\psi_2(3823)$ candidates are reconstructed via $\gamma\chi_{c1}$ decays, with $\chi_{c1} \rightarrow \gamma J/\psi$ and $J/\psi \rightarrow \ell^+\ell^-$ ($\ell = e$ or μ). The π^0 candidates are reconstructed in their $\gamma\gamma$ decays.

2 BESIII detector and Monte Carlo simulation

The BESIII detector is a magnetic spectrometer located at the BEPCII collider [20]. The cylindrical core of the BESIII detector covers 93% of the full solid angle and consists of a helium-based multilayer drift chamber (MDC), a plastic scintillator time-of-flight system (TOF), and a CsI (Tl) electromagnetic calorimeter (EMC), which are all enclosed in a superconducting solenoidal magnet providing a 1.0 T magnetic field. The solenoid is supported by an octagonal flux-return yoke with resistive plate counter muon identification modules interleaved with steel. The charged-particle momentum resolution at $1 \text{ GeV}/c$ is 0.5%, and the dE/dx resolution is 6% for the electrons from Bhabha scattering. The EMC measures photon energies with a resolution of 2.5% (5%) at 1 GeV in the barrel (end cap) region. The time resolution of the TOF barrel part is 68 ps, while that of the end cap part is 110 ps. The end cap TOF system was upgraded in 2015 with multi-gap resistive plate chamber technology, providing a time resolution of 60 ps [21].

A GEANT4-based [22] Monte Carlo (MC) simulation software package is used to optimize event selection criteria, determine detection efficiency, and estimate backgrounds. We generate 100,000 $e^+e^- \rightarrow \pi^0\pi^0\psi_2(3823)$ signal MC events at each CM energy using an EVTGEN [23] phase-space model. The ISR is simulated with KKMC [24], where the cross section of the $e^+e^- \rightarrow \pi^+\pi^-\psi_2(3823)$ process [10] is used as the line shape input. The maximum ISR photon energy is set corresponding to the $4.1 \text{ GeV}/c^2$ production threshold of the $\pi^0\pi^0\psi_2(3823)$ system. Final-State-Radiation is handled with PHOTOS [25].

Backgrounds are investigated using an inclusive MC sample, which includes the production of open-charm processes, the ISR production of vector charmonium(-like) states, and the continuum processes incorporated in KKMC. All particle decays are modelled with EVT-

GEN [23] using branching fractions taken from the Particle Data Group [9] when available, or otherwise modelled with LUNDCHARM [26].

3 Event selection and background study

We select events with two oppositely charged tracks in the polar angle region $|\cos\theta| < 0.93$, where θ is defined with respect to the z -axis (the symmetry axis of the MDC). For each charged track, the distance of closest approach to the interaction point must be less than 10 cm along the beam direction and 1 cm in the plane perpendicular to the beam direction. Charged tracks with momentum greater than 1.0 GeV/ c are assigned as leptons. We make use of the energy depositions in the EMC to identify muons and electrons. The deposited energy in the EMC is required to be less than 0.4 GeV for a muon candidate, while it has to be greater than 1.1 GeV for an electron.

Electromagnetic showers identified as photon candidates must satisfy fiducial shower quality and timing requirements ($0 \leq t \leq 700$ ns). The minimum energy in the EMC is 25 MeV for barrel showers ($|\cos\theta| < 0.80$) and 50 MeV for end cap showers ($0.86 < |\cos\theta| < 0.92$). To exclude showers that originate from charged tracks, the angle subtended by the EMC shower and the position of the closest charged track at the EMC must be greater than 10 degrees as measured from the interaction point. We introduce a partial-reconstruction strategy which has a significantly improved efficiency compared to that of the Ref. [17]. In this strategy, we require only five photons to be reconstructed in each event ($N_\gamma \geq 5$), allowing one missing photon (γ_{miss}). The γ_{miss} can be any one of the six signal photons. The momentum of γ_{miss} is determined from momentum conservation. In addition, we require the number of photons to be $N_\gamma \leq 6$ to suppress the background contribution from the process $\pi^0\pi^0\psi(2S) \rightarrow \pi^0\pi^0\pi^0\pi^0 J/\psi$.

We apply a four-constraint (4C) kinematic fit to the selected events. The invariant mass of the pair of leptons is constrained to the mass of the J/ψ ($m_{J/\psi}$), the mass of the missing photon is constrained to zero, the invariant mass of a pair of photons is constrained to the mass of the π^0 (m_{π^0}), and the same for another pair of photons. The values for $m_{J/\psi}$ and m_{π^0} are taken from the PDG [9]. Since there is more than one possible combination within an event when selecting the photons and reconstructing the π^0 s, we retain the one with the minimum χ^2 from the kinematic fit. Events with $\chi^2 < 15$ are selected for further analysis.

The two remaining photons other than those used for the reconstruction of the π^0 s are boosted to the CM frame of the $\psi_2(3823)$, and the one with a lower energy is considered to originate from the $\psi_2(3823)$ decay, while the other one (with a higher energy) together with the J/ψ candidate is used to reconstruct the χ_{c1} . The mass window of the χ_{c1} candidate is defined as $3.49 < M(\gamma J/\psi) < 3.53$ GeV/ c^2 .

A study of the inclusive MC sample [27] shows that possible backgrounds come from the processes $e^+e^- \rightarrow \eta J/\psi$ with $\eta \rightarrow 3\pi^0$ and $e^+e^- \rightarrow \pi^0\pi^0\psi(2S)$ with $\psi(2S) \rightarrow \pi^0\pi^0 J/\psi$. Background events from $\eta \rightarrow 3\pi^0$ decays are effectively rejected by the invariant mass requirement $M(\gamma\gamma\pi^0\pi^0) > 0.70$ GeV/ c^2 . Background events from $\psi(2S) \rightarrow \pi^0\pi^0 J/\psi$ decays can be suppressed by vetoing the events in the invariant mass region $3.665 < M(\pi^0\pi^0 J/\psi) <$

3.700 GeV/ c^2 . The contributions from other sources, such as $e^+e^- \rightarrow \pi^0\pi^0\pi^0\pi^+\pi^-$, are found to be relatively small. All of the remaining backgrounds only produce a flat distribution in the $\psi_2(3823)$ signal region as shown by the green filled histogram in Figure 1.

4 Measurements of the mass and width of the $\psi_2(3823)$

Figure 1 shows the $M(\gamma\gamma J/\psi)$ distribution for the data from $\sqrt{s} = 4.23$ to 4.70 GeV after the above selection criteria, where obvious $\psi(2S)$ and $\psi_2(3823)$ signal peaks are observed. An unbinned maximum likelihood fit is performed to extract the parameters of the $\psi_2(3823)$ state. The probability density function (PDF) of the signal is represented by the sum of the $\psi(2S)$ and $\psi_2(3823)$ shapes obtained from the MC simulation, each of which is convolved with a Gaussian function to account for the differences in mass resolution between data and MC simulation. The parameters of the $\psi(2S)$ resonance in simulation are taken from the PDG [9]. The mass of the $\psi_2(3823)$ in simulation is set to 3823 MeV/ c^2 and its width is set to zero. The fit parameter σ corresponding to the resolution in Gaussian functions is common for both resonances, while the parameters $\mu_{\psi(2S)}$ and $\mu_{\psi_2(3823)}$ describing the mass shifts are free. The background shape is parameterized as a second-order polynomial function. The fitted mass is $M[\psi_2(3823)] = M[\psi_2(3823)]_{\text{input}} + \mu_{\psi_2(3823)} - \mu_{\psi(2S)} = (3824.5 \pm 2.4 \pm 1.2)$ MeV/ c^2 , where $M[\psi_2(3823)]_{\text{input}} = 3823.0$ MeV/ c^2 is the input mass of the $\psi_2(3823)$ in simulation; $\mu_{\psi_2(3823)} = (1.8 \pm 2.4)$ MeV/ c^2 and $\mu_{\psi(2S)} = (0.3 \pm 1.2)$ MeV/ c^2 are the shift values of the $\psi_2(3823)$ and $\psi(2S)$ shapes, respectively. Here, the first uncertainty in $M[\psi_2(3823)]$ is statistical, which is the uncertainty of $\mu_{\psi_2(3823)}$. The second uncertainty in $M[\psi_2(3823)]$ is the uncertainty of $\mu_{\psi(2S)}$, which is considered to be systematic, since we take the $\psi(2S)$ mass as a reference when measuring the $\psi_2(3823)$ mass. We additionally employ $\psi(2S) \rightarrow \gamma\chi_{c2}$ and $\psi(2S) \rightarrow \eta J/\psi$ data events to increase the $\psi(2S)$ statistics. This reduces the uncertainty of $\mu_{\psi(2S)}$ in the fit, which gives $\mu_{\psi(2S)} = (0.3 \pm 0.9)$ MeV/ c^2 . A more accurate $\psi_2(3823)$ mass $M[\psi_2(3823)] = (3824.5 \pm 2.4 \pm 0.9)$ MeV/ c^2 is therefore achieved.

The total number of $\psi_2(3823)$ signal events extracted from the fit is $N_{\text{total}} = 30.3 \pm 6.8$. A χ^2 -test to the fit quality gives $\chi^2/\text{ndf} = 12.13/26 = 0.47$. According to Wilks's theorem [28], the statistical significance of the $\psi_2(3823)$ signal is estimated to be 6.0σ , by comparing the difference between the log-likelihood values [$\Delta(-2\ln\mathcal{L}) = 40.6$] with and without $\psi_2(3823)$ signal in the fit, and taking into account the change of the number of degrees of freedom ($\Delta\text{ndf} = 2$).

In order to estimate the width of the $\psi_2(3823)$, we slightly modify the fit function described above. We replace the PDF of the $\psi_2(3823)$ signal with a floating-width Breit-Wigner function convolved with Gaussian functions to account for resolution effects. The parameters of the Gaussian functions are fixed according to the study of the resolution in MC simulation, and the resolution difference between data and MC simulation. The $\psi_2(3823)$ width is measured to be $\Gamma[\psi_2(3823)] = (2.9 \pm 5.9)$ MeV, corresponding to an upper limit of 18.8 MeV at the 90% confidence level (including the systematic uncertainty from background shape). Here the upper limit is set based on the Bayesian method [9]. The

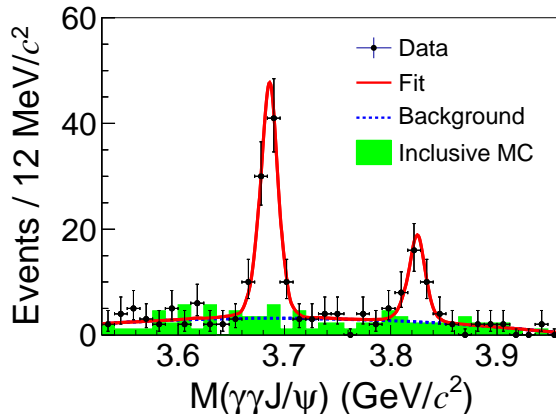


Figure 1. The fit to the $M(\gamma\gamma J/\psi)$ distribution for the data from $\sqrt{s} = 4.23$ to 4.70 GeV. The dots with error bars are the data. The red solid curve is the total fit. The blue dashed curve is the background in the fit and the green filled histogram is the normalized background from the inclusive MC sample.

measured mass and width of the $\psi_2(3823)$ are consistent with the previous measurements by the BESIII [10, 15] and LHCb [16] experiments.

5 Measurement of the ratio of average cross sections

Due to limited statistics, cross sections at each CM energy cannot be effectively measured. Instead, the average cross sections for $e^+e^- \rightarrow \pi^0\pi^0\psi_2(3823)$, denoted by σ_{ave} , and $e^+e^- \rightarrow \pi^+\pi^-\psi_2(3823)$, denoted by σ'_{ave} , are measured as:

$$\sigma_{\text{ave}}^{(\prime)} = \frac{\sum_i \sigma_i^{(\prime)} \mathcal{L}_i (1 + \delta_i) \epsilon_i^{(\prime)}}{\sum_i \mathcal{L}_i (1 + \delta_i) \epsilon_i^{(\prime)}} = \frac{N_{\text{total}}^{(\prime)}}{\sum_i \mathcal{L}_i (1 + \delta_i) \epsilon_i^{(\prime)}} \frac{1}{\mathcal{B}^{(\prime)}}, \quad (5.1)$$

where N_{total} is the total number of observed $\psi_2(3823)$ signal events; σ_i , \mathcal{L}_i , $(1 + \delta_i)$, and ϵ_i are the cross section, luminosity [18], radiative correction factor, and efficiency at the i -th CM energy point, respectively (cf. Table 1); and \mathcal{B} is the product of branching fractions for the chain of decays involved in each process. The unprimed variables are for $e^+e^- \rightarrow \pi^0\pi^0\psi_2(3823)$ and the primed variables are for $e^+e^- \rightarrow \pi^+\pi^-\psi_2(3823)$ with the values taken from Ref. [10]. Note that the luminosities and radiative correction factors are the same for both processes (the minor difference between the numbers in Table 1 and that from Ref. [10] is due to MC statistics). The ratio of average cross sections, $\mathcal{R} \equiv \sigma_{\text{ave}}/\sigma'_{\text{ave}}$, is then calculated as

$$\mathcal{R} = \frac{N_{\text{total}} \sum_i \mathcal{L}_i (1 + \delta_i) \epsilon_i'}{N'_{\text{total}} \sum_i \mathcal{L}_i (1 + \delta_i) \epsilon_i \mathcal{B}^2(\pi^0 \rightarrow \gamma\gamma)}, \quad (5.2)$$

where $\mathcal{B}(\pi^0 \rightarrow \gamma\gamma)$ is the branching fraction of $\pi^0 \rightarrow \gamma\gamma$, and all other branching fractions cancel in the ratio. According to Eq. 5.2, we determine the ratio of average cross sections to be $\mathcal{R} = 0.57 \pm 0.14$, which is consistent with expectations from isospin symmetry ($\mathcal{R} = 0.5$), within uncertainty.

Table 1. The luminosity [18], radiative correction factor and efficiency at each CM energy for the $e^+e^- \rightarrow \pi^0\pi^0\psi_2(3823)$ process.

| \sqrt{s} (GeV) | $\mathcal{L}(\text{pb}^{-1})$ | $(1 + \delta)$ | ϵ |
|------------------|-------------------------------|----------------|------------|
| 4.2263 | 1056.4 | 0.739 | 0.146 |
| 4.2580 | 828.4 | 0.745 | 0.143 |
| 4.2866 | 502.4 | 0.746 | 0.141 |
| 4.3115 | 501.2 | 0.748 | 0.141 |
| 4.3370 | 505.0 | 0.747 | 0.147 |
| 4.3583 | 543.9 | 0.749 | 0.150 |
| 4.3768 | 522.7 | 0.751 | 0.143 |
| 4.3954 | 507.8 | 0.762 | 0.137 |
| 4.4156 | 1043.9 | 0.784 | 0.133 |
| 4.4359 | 569.9 | 0.818 | 0.138 |
| 4.4671 | 111.1 | 0.882 | 0.141 |
| 4.5271 | 112.1 | 1.001 | 0.132 |
| 4.5745 | 48.9 | 1.075 | 0.129 |
| 4.5995 | 586.9 | 1.066 | 0.128 |
| 4.6119 | 103.8 | 0.983 | 0.138 |
| 4.6280 | 521.5 | 0.831 | 0.151 |
| 4.6409 | 552.4 | 0.741 | 0.166 |
| 4.6612 | 529.6 | 0.849 | 0.166 |
| 4.6819 | 1669.3 | 0.985 | 0.152 |
| 4.6988 | 536.5 | 1.053 | 0.143 |

6 Systematic uncertainty

The systematic uncertainties in the $\psi_2(3823)$ mass measurement include those from the absolute mass scale, resolution, signal parameterization, and background shape. In the $\psi_2(3823)$ mass measurement, the $\psi(2S)$ mass is used to calibrate the absolute mass scale, so the uncertainty of the measured $\psi(2S)$ mass is taken as a systematic uncertainty, which is $0.9 \text{ MeV}/c^2$. We change the width of the Gaussian function in the signal PDF by $\pm 1\sigma$ to do the fits, and the largest mass difference to our nominal fit, $0.3 \text{ MeV}/c^2$, is taken as the systematic uncertainty from resolution. The systematic uncertainty from the parameterization of the $\psi_2(3823)$ signal is estimated with different width assumptions. We input a series of $\psi_2(3823)$ widths between zero (which is our nominal value) and its upper limit to generate the MC shapes for the signal PDF constructions, then repeat the fits for the mass measurements. The largest mass difference to our nominal fit, $0.3 \text{ MeV}/c^2$, is taken as a systematic uncertainty. We vary the background shape from a second-order polynomial with floating parameters to a second-order polynomial whose parameters are fixed according to the fit to the inclusive MC sample. The fitted $\psi_2(3823)$ mass difference between these two background assumptions is found to be negligible. Assuming all the sources are

independent, we calculate the total systematic uncertainty by adding them in quadrature, resulting in $1.0 \text{ MeV}/c^2$ for the $\psi_2(3823)$ mass measurement.

The systematic uncertainties in the measurement of the ratio \mathcal{R} include those from the photon efficiency, signal extraction, kinematic fit, MC decay model, χ_{c1} mass window and MC statistics. The systematic uncertainty from the number of good photons requirement $N_\gamma \geq 5$ can be estimated by studying the efficiency difference between data and MC simulation, which is 3.1%. The systematic uncertainty due to the requirement $N_\gamma \leq 6$ originates from the fake-photon-rate difference between data and MC simulation, and this difference is estimated to be 0.1% by studying a control sample of $e^+e^- \rightarrow \pi^0\pi^0 J/\psi$. The signal and background shape parameterizations as discussed in the $\psi_2(3823)$ mass measurement bring 3.6% and 5.0% differences in the $\psi_2(3823)$ signal event yields, which are taken as the systematic uncertainties from signal extraction. A track helix parameter correction method as discussed in Ref. [29] is applied to each MC simulated event during the 4C kinematic fit. The difference in detection efficiencies with and without the corrections, 1.2%, is assigned as the systematic uncertainty from the kinematic fit. The $\psi_2(3823)$ state most likely has quantum numbers $J^{PC} = 2^{--}$ [10], and the $\pi^0\pi^0$ system in $\pi^0\pi^0\psi_2(3823)$ is expected to be dominated by S -wave, such as $f_0(500)$. According to spin-parity conservation, the orbital angular momentum L between $\pi^0\pi^0$ and $\psi_2(3823)$ is therefore 2. We perform MC simulation of the $e^+e^- \rightarrow \pi^0\pi^0\psi_2(3823)$ process with $L = 2$ between $\pi^0\pi^0$ and $\psi_2(3823)$. The efficiency difference between this model and the nominal three-body phase-space model, 1.0%, is taken as the systematic uncertainty from the MC decay model. Using a control sample from the process $e^+e^- \rightarrow \pi^+\pi^-\psi(2S) \rightarrow \pi^+\pi^-\gamma\chi_{c1}$, we estimate the systematic uncertainty due to the χ_{c1} mass window requirement to be 1.1%. The uncertainty from the MC sample size is 0.8%. We change the input cross section line shape from a two-resonance interpretation to an alternative single-resonance interpretation, as described in Ref. [10], and find the variation among the calculated ratios \mathcal{R} is negligible. The systematic uncertainties from luminosity, lepton efficiency, branching fractions $\mathcal{B}(\chi_{c1} \rightarrow \gamma J/\psi)$ and $\mathcal{B}(J/\psi \rightarrow \ell^+\ell^-)$ cancel. The uncertainty from the quoted branching fraction $\mathcal{B}^2(\pi^0 \rightarrow \gamma\gamma)$ is negligible [9]. The systematic uncertainties inherent only from the charged channel $e^+e^- \rightarrow \pi^+\pi^-\psi_2(3823)$ [10] are estimated to be 5.3% in total. Assuming all the sources are independent and there is no correlation between neutral and charged channels for the above systematic uncertainties, we calculate the total systematic uncertainty by adding them in quadrature, resulting in 8.9% for the measurement of the ratio \mathcal{R} .

7 Summary and discussion

In summary, by using a data sample corresponding to an integrated luminosity of 11.3 fb^{-1} collected with the BESIII detector at CM energies from 4.23 to 4.70 GeV, the process $e^+e^- \rightarrow \pi^0\pi^0\psi_2(3823)$ is observed for the first time. The ratio of average cross sections for $e^+e^- \rightarrow \pi^0\pi^0\psi_2(3823)$ over $e^+e^- \rightarrow \pi^+\pi^-\psi_2(3823)$ is measured to be $\mathcal{R} \equiv \sigma_{\text{ave}}/\sigma'_{\text{ave}} = 0.57 \pm 0.14 \pm 0.05$, which agrees with the expectation from isospin symmetry. This result supports the di-pion transition of the Y -states to $\psi_2(3823)$ observed in

$e^+e^- \rightarrow \pi^+\pi^-\psi_2(3823)$ [10], though currently we do not have enough statistics to measure the CM energy dependent cross sections of $e^+e^- \rightarrow \pi^0\pi^0\psi_2(3823)$.

The mass of the $\psi_2(3823)$ is measured to be $M[\psi_2(3823)] = (3824.5 \pm 2.4 \pm 1.0)$ MeV/ c^2 , which is in agreement with the previous measurements [10, 14–16]. Due to the limited statistics, an upper limit is given to the width of $\psi_2(3823)$, which is $\Gamma[\psi_2(3823)] < 18.8$ MeV at the 90% confidence level. According to an angular distribution study of the $\psi_2(3823)$ from the process $e^+e^- \rightarrow \pi^+\pi^-\psi_2(3823)$ at BESIII [10], the $\psi_2(3823)$ is likely a state with quantum numbers $J^{PC} = 2^{--}$ assuming the $\pi^+\pi^-$ system is dominated by $f_0(500)$. Since the $\rho^0 \rightarrow \pi^0\pi^0$ decay is forbidden, the observation of $e^+e^- \rightarrow \pi^0\pi^0\psi_2(3823)$ thus further confirms that the $\pi\pi$ system in $e^+e^- \rightarrow \pi\pi\psi_2(3823)$ comes from $f_0(500)$ decay instead of the ρ^0 . It therefore supports the $J^{PC} = 2^{--}$ assignment for the $\psi_2(3823)$.

Acknowledgments

The BESIII collaboration thanks the staff of BEPCII and the IHEP computing center for their strong support. This work is supported in part by National Key R&D Program of China under Contracts Nos. 2020YFA0406300, 2020YFA0406400; National Natural Science Foundation of China (NSFC) under Contracts Nos. 11975141, 11635010, 11735014, 11835012, 11935015, 11935016, 11935018, 11961141012, 12022510, 12025502, 12035009, 12035013, 12192260, 12192261, 12192262, 12192263, 12192264, 12192265; the Chinese Academy of Sciences (CAS) Large-Scale Scientific Facility Program; Joint Large-Scale Scientific Facility Funds of the NSFC and CAS under Contract No. U1832207; 100 Talents Program of CAS; Project ZR2022JQ02 supported by Shandong Provincial Natural Science Foundation; The Institute of Nuclear and Particle Physics (INPAC) and Shanghai Key Laboratory for Particle Physics and Cosmology; ERC under Contract No. 758462; European Union’s Horizon 2020 research and innovation programme under Marie Skłodowska-Curie grant agreement under Contract No. 894790; German Research Foundation DFG under Contracts Nos. 443159800, Collaborative Research Center CRC 1044, GRK 2149; Istituto Nazionale di Fisica Nucleare, Italy; Ministry of Development of Turkey under Contract No. DPT2006K-120470; National Science and Technology fund; National Science Research and Innovation Fund (NSRF) via the Program Management Unit for Human Resources & Institutional Development, Research and Innovation under Contract No. B16F640076; STFC (United Kingdom); Suranaree University of Technology (SUT), Thailand Science Research and Innovation (TSRI), and National Science Research and Innovation Fund (NSRF) under Contract No. 160355; The Royal Society, UK under Contracts Nos. DH140054, DH160214; The Swedish Research Council; U. S. Department of Energy under Contract No. DE-FG02-05ER41374.

References

- [1] S. L. Olsen, T. Skwarnicki and D. Zieminska, *Nonstandard heavy mesons and baryons: Experimental evidence*, *Rev. Mod. Phys.* **90** (2018) 015003.
- [2] N. Brambilla et al., *The XYZ states: experimental and theoretical status and perspectives*, *Phys. Rept.* **873** (2020) 1.

- [3] BaBar collaboration, *Observation of a broad structure in the $\pi^+\pi^-J/\psi$ mass spectrum around $4.26\text{ GeV}/c^2$* , *Phys. Rev. Lett.* **95** (2005) 142001.
- [4] Belle collaboration, *Measurement of $e^+e^- \rightarrow \pi^+\pi^-J/\psi$ cross-section via initial state radiation at Belle*, *Phys. Rev. Lett.* **99** (2007) 182004.
- [5] BaBar collaboration, *Evidence of a broad structure at an invariant mass of $4.32\text{ GeV}/c^2$ in the reaction $e^+e^- \rightarrow \pi^+\pi^-\psi(2S)$ measured at BaBar*, *Phys. Rev. Lett.* **98** (2007) 212001.
- [6] Belle collaboration, *Observation of Two Resonant Structures in $e^+e^- \rightarrow \pi^+\pi^-\psi(2S)$ via Initial State Radiation at Belle*, *Phys. Rev. Lett.* **99** (2007) 142002.
- [7] BaBar collaboration, *Study of the reaction $e^+e^- \rightarrow \psi(2S)\pi^-\pi^-$ via initial-state radiation at BaBar*, *Phys. Rev. D* **89** (2014) 111103.
- [8] E. Eichten, K. Gottfried, T. Kinoshita, K. D. Lane and T. M. Yan, *Charmonium: The Model*, *Phys. Rev. D* **17** (1978) 3090; *Phys. Rev. D* **21** (1980) 313.
- [9] Particle Data Group, *Review of Particle Physics*, *PTEP* **2022** (2022) 083C01.
- [10] BESIII collaboration, *Observation of resonance structures in $e^+e^- \rightarrow \pi^+\pi^-\psi_2(3823)$ and mass measurement of $\psi_2(3823)$* , *Phys. Rev. Lett.* **129** (2022) 102003.
- [11] J. J. Aubert et al., *Experimental Observation of a Heavy Particle J* , *Phys. Rev. Lett.* **33** (1974) 1404; J. E. Augustin et al., *Discovery of a Narrow Resonance in e^+e^- Annihilation*, *Phys. Rev. Lett.* **33** (1974) 1406.
- [12] N. Brambilla et al., *Heavy Quarkonium: Progress, Puzzles, and Opportunities*, *Eur. Phys. J. C* **71** (2011) 1534.
- [13] E705 collaboration, *Search for hidden charm resonance states decaying into J/ψ or ψ' plus pions*, *Phys. Rev. D* **50** (1994) 4258.
- [14] Belle collaboration, *Evidence of a new narrow resonance decaying to $\chi_{c1}\gamma$ in $B \rightarrow \chi_{c1}\gamma K$* , *Phys. Rev. Lett.* **111** (2013) 032001.
- [15] BESIII collaboration, *Observation of the $\psi(1^3D_2)$ state in $e^+e^- \rightarrow \pi^+\pi^-\gamma\chi_{c1}$ at BESIII*, *Phys. Rev. Lett.* **115** (2015) 011803.
- [16] LHCb collaboration, *Study of the $\psi_2(3823)$ and $\chi_{c1}(3872)$ states in $B^+ \rightarrow (J/\psi\pi^+\pi^-)K^+$ decays*, *JHEP* **08** (2020) 123.
- [17] BESIII collaboration, *Search for new decay modes of the $\psi_2(3823)$ and the process $e^+e^- \rightarrow \pi^0\pi^0\psi_2(3823)$* , *Phys. Rev. D* **103** (2021) L091102.
- [18] BESIII collaboration, *Measurement of the center-of-mass energies at BESIII via the di-muon process*, *Chin. Phys. C* **40** (2016) 063001; BESIII collaboration, *Measurements of the center-of-mass energies of collisions at BESIII*, *Chin. Phys. C* **45** (2021) 103001; BESIII collaboration, *Luminosities and energies of e^+e^- collision data taken between $\sqrt{s} = 4.612\text{ GeV}$ and 4.946 GeV at BESIII*, [arXiv:2205.04809].
- [19] BESIII collaboration, *Design and Construction of the BESIII Detector*, *Nucl. Instrum. Meth. A* **614** (2010) 345.
- [20] C. Yu et al., *BEPCII Performance and Beam Dynamics Studies on Luminosity*, [doi:10.18429/JACoW-IPAC2016-TUYA01].
- [21] X. Li et al., *Study of MRPC technology for BESIII endcap-TOF upgrade*, *Radiat. Detect. Technol. Methods* **1** (2017) 13; Y. X. Guo et al., *The study of time calibration for upgraded*

- end cap TOF of BESIII, Radiat. Detect. Technol. Methods* **1** (2017) 15; P. Cao et al., *Design and construction of the new BESIII endcap Time-of-Flight system with MRPC Technology, Nucl. Instrum. Meth. A* **953** (2020) 163053.
- [22] GEANT4 collaboration, *GEANT4—a simulation toolkit, Nucl. Instrum. Meth. A* **506** (2003) 250.
- [23] D. J. Lange, *The EvtGen particle decay simulation package, Nucl. Instrum. Meth. A* **462** (2001) 152; R. G. Ping, *Event generators at BESIII, Chin. Phys. C* **32** (2008) 599.
- [24] S. Jadach, B. F. L. Ward and Z. Was, *The Precision Monte Carlo event generator KK for two fermion final states in e^+e^- collisions, Comput. Phys. Commun.* **130** (2000) 260; S. Jadach, B. F. L. Ward and Z. Was, *Coherent exclusive exponentiation for precision Monte Carlo calculations, Phys. Rev. D* **63** (2001) 113009.
- [25] E. Richter-Was, *QED bremsstrahlung in semileptonic B and leptonic tau decays, Phys. Lett. B* **303** (1993) 163; P. Golonka and Z. Was, *PHOTOS Monte Carlo: A Precision tool for QED corrections in Z and W decays, Eur. Phys. J. C* **45** (2006) 97.
- [26] J. C. Chen, G. S. Huang, X. R. Qi, D. H. Zhang and Y. S. Zhu, *Event generator for J/ψ and $\psi(2S)$ decay, Phys. Rev. D* **62** (2000) 034003; R. L. Yang, R. G. Ping and H. Chen, *Tuning and Validation of the Lundcharm Model with J/ψ Decays, Chin. Phys. Lett.* **31** (2014) 061301.
- [27] X. Y. Zhou, S. X. Du, G. Li and C. P. Shen, *TopoAna: A generic tool for the event type analysis of inclusive Monte-Carlo samples in high energy physics experiments, Comput. Phys. Commun.* **258** (2021) 107540.
- [28] S. S. Wilks, *The Large-Sample Distribution of the Likelihood Ratio for Testing Composite Hypotheses, Annals Math. Statist.* **9** (1938) 60.
- [29] BESIII collaboration, *Search for hadronic transition $\chi_{cJ} \rightarrow \eta_c \pi^+ \pi^-$ and observation of $\chi_{cJ} \rightarrow K \bar{K} \pi \pi$, Phys. Rev. D* **87** (2013) 012002.